Spin Crossover

DOI: 10.1002/anie.200802906

Towards the Ultimate Size Limit of the Memory Effect in Spin-Crossover Solids**

Joulia Larionova, Lionel Salmon, Yannick Guari, Alexeï Tokarev, Karine Molvinger, Gábor Molnár, and Azzedine Bousseksou**

Dedicated to Professor Jan Reedijk on the occasion of his 65th birthday

The phenomenon of spin crossover (SCO) between high-spin (HS) and low-spin (LS) states of $3d^4$–$3d^7$ transition-metal complexes has attracted much interest.[1] Although the origin of the spin-crossover phenomenon is purely molecular, the macroscopic behavior of these systems in the solid state is strongly influenced by short- and long-range interactions (of mainly elastic origin) between the transition-metal ions, giving rise to remarkable cooperative phenomena, such as first-order phase transitions.[2] One of the most interesting open questions in this research field concerns the effect of size reduction on the cooperativity and on the relevant physical properties. Notably, the hysteresis, which in certain cases accompanies the thermal spin transition, is considered to be an important property, as it confers a memory effect on these systems. As was suggested by Kahn and Martinez,[3] this phenomenon might be used for information storage. The same authors have estimated from statistical considerations that approximately 10^3 strongly interacting metal ions (i.e. comprising a particle with a diameter of a few nanometers) should be the approximate lower size limit for which an SCO solid might still exhibit hysteresis. The size dependence of the hysteresis width has also been investigated by Kawamoto and Abe on a model system taking into account only short-range interactions,[4] but the complexity of the elastic interactions in real systems and the poor knowledge of the relevant lattice properties (and their size dependence) makes it very difficult to reliably predict the interaction energies and hence the hysteresis width.

To our knowledge, the first results concerning the size-reduction effect in SCO systems was reported by Létard et al.[5,6] These authors claimed the observation of a thermal hysteresis loop in nanoparticles $[Fe(NH_2trz)_3]Br_2$ of approximately 60–200 nm size (NH_2trz = 4-amino-1,2,4-triazole). More recently, Coronado et al. have succeeded in synthesizing nanoparticles of $[Fe(Htrz)_2(trz)](BF_4)$ with a mean statistical size of approximately 15 nm, which exhibited a hysteresis loop 43 K wide.[7] At the same time, some of us reported an alternative method for the fabrication of nano-objects (down to 30 nm) exhibiting SCO properties based on the lithographic patterning of thin films.[8,9] Such ordered arrays of SCO micro- and nanostructures are particularly interesting for potential applications of this phenomenon, but in the sub-micrometer range it is rather challenging to characterize their structure and physical properties, owing to the small signals. Moreover, it is difficult to obtain nano-objects with sizes below 10 nm by means of lithographic techniques. This range is, however, accessible by chemical methods, which have the further advantage of allowing the synthesis of a large number of particles, and thus their physical characterization becomes feasible by standard averaging techniques, such as magnetometry.

Herein, we report the synthesis and study of ultra-small monodisperse nanoparticles of the 3D spin crossover coordination polymer $[Fe(pyrazine)\{Ni(CN)_4\}]$,[10] obtained using the biopolymer chitosan as matrix. It should be noted that investigations on the synthesis of cyano-bridged coordination polymers at the nanoscale level have attracted a great deal of attention in recent years, and numerous methods have been reported, including the use of reverse micelles,[11] ionic liquids,[12] various ligands[13] and polymers[14] as stabilizing agents, biopolymers,[15] amorphous[16] and mesostructured silica,[17] as well as porous alumina electrode[18] as matrixes. Some of us recently published the synthesis and study of magnetic cyano-bridged metallic coordination polymer nanoparticles $M^{n+}/[Fe(CN)_6]^{3-}$ with controlled size of 2–3 nm using chitosan beads as matrix.[19] The advantages of this approach consist of 1) the possibility to covalently anchor the cyano-bridged metallic network at the reactive functional amino groups of the chitosan; 2) the possibility to afford ultra-small nanoparticles (less than 10 nm); 3) the water solubility of the chitosan matrix that permits removal of the nanoparticles from the matrix.

[*] Dr. J. Larionova, Dr. Y. Guari, Dr. A. Tokarev
Institut Charles Gerhardt Montpellier
UMR5253, Chimie Moléculaire et Organisation du Solide
Université Montpellier II
Place E. Bataillon, 34095 Montpellier Cx5 (France)
Fax: (+33) 4-6714-3852
E-mail: joulia@univ-montp2.fr
Dr. L. Salmon, Dr. G. Molnár, Dr. A. Bousseksou
Laboratoire de Chimie de Coordination, UPR8241
205, route de Narbonne, 31077 Toulouse Cx4 (France)
Fax: (+33) 5-6155-3003
E-mail: boussek@lcc-toulouse.fr
Dr. K. Molvinger
Institut Charles Gerhardt Montpellier, UMR5253
Matériaux Avancés pour la Catalyse et la Santé
Ecole Normale Supérieure de Chimie de Montpellier
8 rue de l'école Normale, 34296 Montpellier Cx5 (France)

[**] The authors thank Mme Corine Reibel (LPMC, Montpellier, France) for magnetic measurements. Financial supports from the CNRS, the Université Montpellier II, the ANR NANOMOL project and the European Network of Excellence MAGMANET are acknowledged.

Supporting information for this article is available on the WWW under http://dx.doi.org/10.1002/anie.200802906.

InterScience DISCOVER SOMETHING GREAT
© 2008 Wiley-VCH Verlag GmbH & Co. KGaA, Weinheim

On the basis of these results, coordination polymer nanoparticles of [Fe(pyrazine){Ni(CN)$_4$}] were obtained in a chitosan matrix by adapting the multilayer sequential assembly (MSA) process developed for the preparation of the corresponding thin film.[8,9] Consecutive treatments of the pristine chitosan beads with methanolic solutions of Fe(BF$_4$)$_2$·6H$_2$O, pyrazine, and (N(C$_4$H$_9$)$_4$)$_2$[Ni(CN)$_4$] were carried out (Scheme 1) and repeated twice. At each step of the

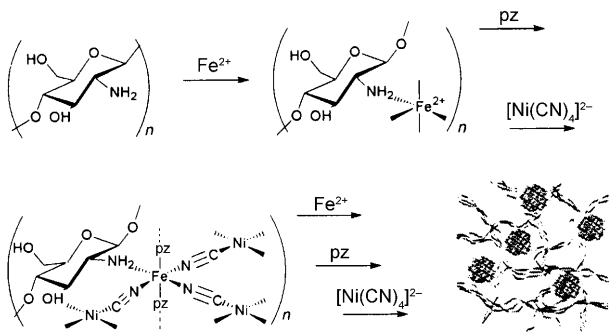

Scheme 1. Schematic representation of the synthesis of [Fe(pyrazine)]$^{2+}$/[Ni(CN)$_4$]$^{2-}$/chitosan nanocomposite beads. pz = pyrazine.

treatment, the chitosan beads were thoroughly washed with methanol to remove unanchored species. The obtained nanocomposite beads (Figure S1 in the Supporting Information) were dried in vacuo and heated at 110 °C to remove the solvent. Energy dispersive X-ray analysis (EDX) showed that Fe and Ni contents (Ni/Fe = 1.8) are constant through the whole chitosan bead (Figure S2 in the Supporting Information). This ratio is in agreement with the results of the elemental analyses.

The as-obtained nanocomposite beads have the orange color of the corresponding bulk counterpart (absorption centered around 467 nm, Figure S3 in the Supporting Information). Besides the characteristic bands of the chitosan, IR spectra of the nanocomposites beads clearly show bands at 2161, 2143, and 2122 cm^{-1} corresponding to the stretching vibrations of the bridging cyano groups, which can also be found in the IR spectra of the bulk analogues.[20]

The transmission electron microscopy (TEM) measurements performed on the nanocomposite beads clearly show the presence of non-aggregated uniform nanoparticles homogeneously dispersed within the chitosan matrix (Figure 1 a). The histogram of the nanoparticle size distribution shows a mean size (standard deviation) of 3.8(0.8) nm (Figure 1 a, inset). To demonstrate the presence of non-aggregated nanoparticles, TEM measurements were also performed after the chitosan matrix was solubilized in an acidic aqueous solution (pH 4.75). The TEM micrograph of this sample shows non-aggregated uniformly sized spherical nanoparticles with a size distribution centered at 3.8(1.1) nm (Figure 1 b) As was mentioned previously, a chitosan shell surrounding the inorganic core of the nanoparticles is expected still to be present at this stage.[19]

The magnetic properties of the [Fe(pyrazine)]$^{2+}$/[Ni(CN)$_4$]$^{2-}$/chitosan nanoparticles were measured in the

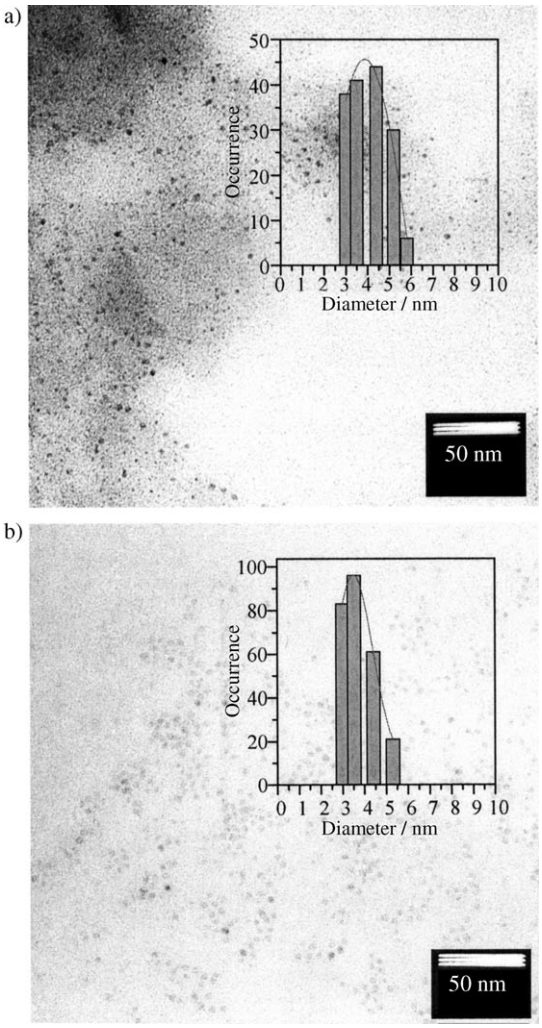

Figure 1. TEM images of [Fe(pyrazine){Ni(CN)$_4$}] nanoparticles a) within the chitosan beads and b) after solubilization of the chitosan matrix in water. The insets show size distribution histograms of the nanoparticles.

100–350 K range with an applied field of 10000 Oe at slow heating and cooling rates (0.5 K min^{-1}). The temperature dependence of the magnetization (Figure 2) indicates a spin transition between the high spin (HS) and low spin (LS) forms of the ferrous ions with a thermal hysteresis loop. The transition temperatures in the heating and cooling modes are circa $T_{1/2}\uparrow = 290$ K and $T_{1/2}\downarrow = 280$ K, respectively. This result points clearly to the first-order nature of the thermal phase transition in the nanoparticles.

The properties of the solvent-free microcrystalline powder form of [Fe(pyrazine){Ni(CN)$_4$}] have been reported, and a considerably larger hysteresis loop (30 K) was observed around the same temperature.[8] The difference in the hysteresis size and the difference in the abruptness of the phase transition between the powdered sample and the nanoparticles can probably be linked to the combined effect of size reduction as well as the increased number of defects (which appear chiefly because of the significantly higher surface-to-volume ratio), leading to the concomitant decrease of the cooperativity of the system.

 © 2008 Wiley-VCH Verlag GmbH & Co. KGaA, Weinheim

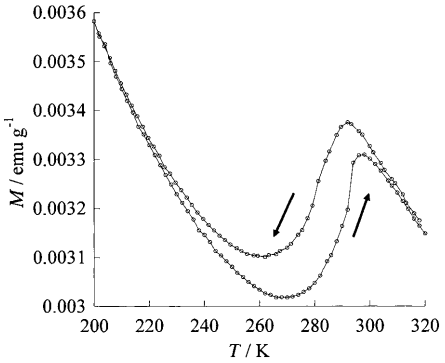

Figure 2. Temperature dependence of the magnetization measured for the nanocomposite beads under an applied field of 10000 Oe at heating and cooling rates of 0.5 K min^{-1}. Lines are to guide the eyes.

Figure 3 shows a comparison of Raman spectra of the $[Fe(pyrazine)]^{2+}/[Ni(CN)_4]^{2-}$/chitosan nanoparticles and microcrystalline powder of $[Fe(pyrazine)\{Ni(CN)_4\}]$ at room temperature. Owing to the very weak intensity of the Raman scattering from the chitosan matrix, the comparison of the

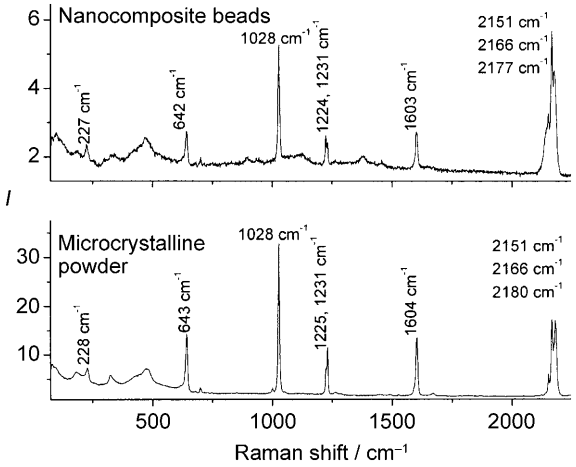

Figure 3. Raman spectra of the nanocomposite beads and of the microcrystalline powder of $[Fe(pyrazine)\{Ni(CN)_4\}]$ recorded at 295 K.

two spectra is straightforward and confirms clearly that the structure and composition of the nanoparticles is similar to the bulk analogue. (Small spectral differences can, however, be noticed and should be related to the chitosan matrix as well as to various defects, such as surface states and trapped solvent molecules.) Furthermore, the Raman spectra of the nanoparticles at 320 and 280 K (Figure S4 in the Supporting Information) reveal a shift of the in-plane bending mode of the pyrazine ring from 645 to 675 cm^{-1} upon cooling, which is a characteristic sign of the HS-to-LS spin-state change,[20] thus corroborating the results of the magnetic measurements. (See also the temperature dependence of the Raman intensity and the color change of the nanocomposite beads in the Supporting Information, Figures S5 and S6.)

The quantitative determination of the fraction of iron centers involved in the spin transition is difficult from the magnetic or Raman data obtained on such a complex system as the nanocomposite beads. To this end, we recorded the ^{57}Fe Mössbauer spectra of the $[Fe(pyrazine)]^{2+}/[Ni(CN)_4]^{2-}$/chitosan nanocomposite beads at various temperatures. Representative Mössbauer spectra recorded in the cooling mode at 310 and 220 K are shown in Figure 4, and values of the Mössbauer

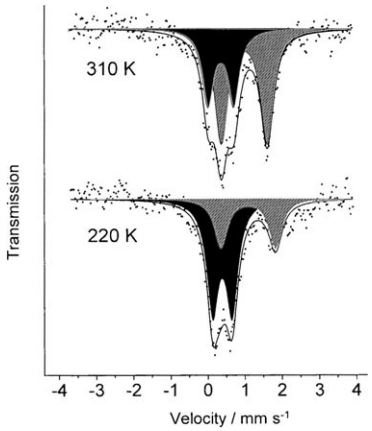

Figure 4. Selected ^{57}Fe Mössbauer spectra of the nanocomposite beads acquired at 310 and 220 K. The solid lines represent fitted curves. The HS Fe^{II} doublet is shown in shaded gray, the LS Fe^{II} doublet in black.

parameters obtained by least-squares fitting of the spectra are gathered in Table 1 for each spectrum. At 310 K the Mössbauer spectrum consists of two quadrupole-split doublets. One doublet (isomer shift $\delta = 1.02(1)$ mm s^{-1}, quadrupole spitting $\Delta E_Q = 1.23(2)$ mm s^{-1}) is typical of a HS iron(II) center ($S = 2$), and the other ($\delta = 0.39(2)$ mm s^{-1}, $\Delta E_Q = 0.70(4)$ mm s^{-1}) corresponds to a low spin iron(II) species ($S = 0$); the relative areas are 62 and 38%, respectively. When the sample is cooled to 220 K, the area of the HS doublet decreases and, conversely, the area of the LS doublet increases. The residual high spin doublet at 220 K accounts for approximately 33% of the total area, which does not change significantly upon further cooling to 80 K. These

Table 1: Hyperfine Mössbauer parameters (and their statistical errors) of iron(II) ions in the nanocomposite beads at various temperatures.[a]

T [K]	HS doublet				LS doublet			
	δ [mm s^{-1}]	ΔE_Q [mm s^{-1}]	$\Gamma/2$ [mm s^{-1}]	Area [%]	δ [mm s^{-1}]	ΔE_Q [mm s^{-1}]	$\Gamma/2$ [mm s^{-1}]	Area [%]
310	1.02(1)	1.23(2)	0.21(2)	62(6)	0.39(2)	0.70(4)	0.19(3)	38(4)
293	1.05(1)	1.22(2)	0.22(2)	60(5)	0.41(2)	0.66(3)	0.20(2)	40(4)
220	1.09(2)	1.45(5)	0.2	33(4)	0.39(1)	0.52(2)	0.18	67(3)
80	1.35(2)	2.09(3)	0.2	34(3)	0.40(1)	0.58(3)	0.29(2)	66(3)

[a] δ, ΔE_Q, and Γ stand for the isomer shift, the quadrupole splitting, and the half-height line width, respectively. Parameters for which no error is listed were fixed during the fit.

 © 2008 Wiley-VCH Verlag GmbH & Co. KGaA, Weinheim

results are in agreement with those obtained by magnetic measurements and also reveal that approximately 1/3 of iron ions inside the nanoparticles are involved in the thermal phase transition. The small thermally active fraction can be related to the small size of the nanoparticles (3–5 nm). For example, the percentage of the iron atoms localized at the surface of 4 nm diameter nanoparticles is approximately 60–70 % (taking into account the ca. 400 Å^3 unit cell volume[21]). It can therefore be tentatively suggested that the different environments around the iron atoms at the surface, in comparison with those inside the nanoparticles, can lead to the loss of the SCO property. Of course, other effects (size distribution, structural disorder, solvent guest molecules, etc.) may also significantly affect the measured averaged properties, and a more detailed investigation as a function of the particle size and size distribution will be necessary to evaluate the role of the different parameters.

In summary, we describe herein for the first time the synthesis of cyano-bridged coordination polymer nanoparticles $[Fe(pyrazine)]^{2+}/[Ni(CN)_4]^{2-}$/chitosan by using porous chitosan beads as matrix. We show that the porous chitosan beads containing amino functionalities allow the growth of ultra-small nanoparticles (3.8 nm) with a narrow size distribution. The study of the physical properties of these nanocomposite beads reveals that approximately 1/3 of the iron(II) ions in the nanoparticles undergo a cooperative thermal spin transition with a hysteresis loop. This study provides thus the first real experimental confirmation of the prediction by Kahn that the lower size limit for the observation of a cooperative spin crossover phenomenon (at room temperature) should be around a few nanometers.[3] We believe that this result should encourage research for technological applications of SCO materials, and it also opens interesting perspectives for fundamental studies of phase transitions.[23]

Experimental Section

All of the chemical reagents used in these experiments were analytical grade. The chitosan beads were prepared using a published procedure,[22] and the preparation of nanocomposite beads was performed under argon atmosphere in a Schlenk tube. $Fe(BF_4)_2{\cdot}6H_2O$ (0.6 mmol, 0.200 g) in methanol (20 mL) was added to the chitosan beads (0.090 g), and the suspension was shaken for 48 h. The solution was removed, and the chitosan beads were washed three times with dry methanol (20 ml). Then, a solution of pyrazine (0.3 mmol, 0.024 g) in methanol (10 mL) was added to the chitosan beads, and the solution was shaken for 48 h. The chitosan beads were removed and washed with methanol. Finally, the chitosan beads were treated the same way with a solution of tetrabutylammonium tetracyanonickelate(II) (0.3 mmol, 0.200 g) in methanol (20 mL), removed, and washed with methanol. At this stage of the treatment, the chitosan beads change their color to orange. Such consecutive treatments with the iron salt, pyrazine, and tetracyanonickelate precursors were repeated once again. The elemental analyses (%) gave Fe 5.80 and Ni 9.55, that is, an atomic ratio of Ni/Fe = 1.65. The nanocomposite beads were then immersed in an acetic acid/sodium acetate buffer solution (pH 4.75) until the chitosan beads were dissolved. The resulting solution was centrifuged to recover the supernatant solution containing the $[Fe(pyrazine)]^{2+}/[Ni(CN)_4]^{2-}$/chitosan nanoparticles.

IR spectra were recorded on a Perkin–Elmer 1600 spectrometer with a 4 cm^{-1} resolution using KBr pellets. UV/Vis spectra were also recorded on KBr disks by means of a Cary 5E spectrometer. Elemental analyses were performed by the Service Central d'Analyse (CNRS, Vernaison, France). Magnetic susceptibility data were collected with a Quantum Design MPMS-XL SQUID magnetometer at various heating and cooling rates between 0.5 and 3 K min^{-1} in the temperature range 100–350 K and at a magnetic field of 10 kOe. ^{57}Fe Mössbauer spectra were recorded using a conventional constant-acceleration-type spectrometer equipped with a 50 mCi ^{57}Co source and a flow-type, liquid-nitrogen cryostat. Spectra of the powder sample (ca. 20 mg) were recorded between 80 and 310 K with typical acquisition times between three and five days. Least-squares fittings of the Mössbauer spectra have been carried out with the assumption of Lorentzian line shapes using the Recoil software package. Samples for TEM measurements were prepared using ultramicrotomy techniques from resin-embedded powder or from drops of the water solutions deposited onto copper grids. TEM measurements were carried out at 100 kV using a JEOL 1200 EXII microscope. The nanoparticle size distribution histograms were determined using enlarged TEM micrographs taken at magnification of × 50k. A large number of nanoparticles were counted to obtain a size distribution with good statistical reliability. Variable-temperature Raman spectra were collected using a LabRAM-HR (Jobin Yvon) Raman spectrometer. The 632.8 nm line of a 17 mW He–Ne laser was used as the excitation source, and the exciting radiation was directed through a neutral density filter (OD = 2) to avoid sample heating. Samples were enclosed in nitrogen atmosphere on the cold finger of a THMS600 (Linkam) liquid-nitrogen cryostage.

Received: June 18, 2008
Published online: September 18, 2008

Keywords: chitosan · coordination polymers · cyanides · nanoparticles · spin crossover

[1] P. Gütlich, A. Hauser, H. Spiering, *Angew. Chem.* **1994**, *106*, 2109 – 2141; *Angew. Chem. Int. Ed. Engl.* **1994**, *33*, 2024 – 2054.
[2] H. Spiering, *Top. Curr. Chem.* **2004**, *235*, 171 – 195.
[3] O. Kahn, C. J. Martinez, *Science* **1998**, *279*, 44 – 48.
[4] T. Kawamoto, S. Abe, *Chem. Commun.* **2005**, 3933 – 3935.
[5] J.-F. Létard, P. Guionneau, L. Goux-Capes, *Top. Curr. Chem.* **2004**, *235*, 221 – 249.
[6] J. F. Létard, O. Nguyen, N. Daro, Patent FR2894581, **2007**.
[7] E. Coronado, J. R. Galán-Mascarós, M. Monrabal-Capilla, J. Garciía-Martínez, P. Pardo-Ibánez, *Adv. Mater.* **2007**, *19*, 1359 – 1361.
[8] S. Cobo, G. Molnar, J. A. Real, A. Bousseksou, *Angew. Chem.* **2006**, *118*, 5918; *Angew. Chem. Int. Ed.* **2006**, *45*, 5786 – 5789.
[9] G Molnár, S. Cobo, J. A. Real, F. Carcenac, E. Daran, C. Vieu, A. Bousseksou, *Adv. Mater.* **2007**, *19*, 2163 – 2167.
[10] a) V. Niel, J. M. Martinez-Agundo, M. Carmen Munoz, A. B. Gaspar, J. A. Real, *Inorg. Chem.* **2001**, *40*, 3838 – 3839.
[11] a) S. Vaucher, M. Li, S. Mann, *Angew. Chem.* **2000**, *112*, 1863 – 1866; *Angew. Chem. Int. Ed.* **2000**, *39*, 1793 – 1796; b) S. Vaucher, J. Fielden, M. Li, E. Dujardin, S. Mann, *Nano Lett.* **2002**, *2*, 225 – 229; c) L. Catala, T. Gacoin, J.-P. Boilot, E. Rivière, C. Paulsen, E. Lhotel, T. Mallah, *Adv. Mater.* **2003**, *15*, 826 – 829.
[12] a) G. Clavel, J. Larionova, Y. Guari, C. Guérin, *Chem. Eur. J.* **2006**, *12*, 3798 – 3804; b) J. Larionova, Y. Guari, H. Sayegh, C. Guérin, *Inorg. Chim. Acta* **2007**, *360*, 3829 – 3836; c) J. Larionova, Y. Guari, A. Tokarev, E. Chelebaeva, C. Sangregorio, A. Caneschi, Ch. Guérin, *Inorg. Chim. Acta* **2008**, *361*, 3988 – 3996.
[13] E. Chelebaeva, Y. Guari, J. Larionova, A. Trifonov, C. Guérin, *Chem. Mater.* **2008**, *20*, 1367 – 1375.
[14] a) T. Uemura, S. Kitagawa, *J. Am. Chem. Soc.* **2003**, *125*, 7814 – 7815; b) D. M. DeLongchamp, P. T. Hammond, *Adv. Funct. Mater.* **2004**, *14*, 224 – 232; c) L. Catala, A. Gloter, O. Stephan, G.

 © 2008 Wiley-VCH Verlag GmbH & Co. KGaA, Weinheim

Rogez, T. Mallah, *Chem. Commun.* **2006**, 1018 – 1020; d) D. Brinzei, L. Catala, N. Louvain, G. Rogez, O. Stéphan, A. Gloter, T. Mallah, *J. Mater. Chem.* **2006**, *16*, 2593 – 2599; e) L. Catala, C. Mathonière, A. Gloter, O. Stephan, T. Gacoin, J.-P. Boilot, T. Mallah, *Chem. Commun.* **2005**, 746 – 748; f) F. A. Frye, D. M. Pajerowski, N. E. Anderson, J. Long, J.-H. Park, M. W. Meisel, D. R. Talham, *Polyhedron* **2007**, *26*, 2273 – 2275; g) D. M. Pajerowski, F. A. Frye, D. R. Talham, M. W. Meisel, *New J. Phys.* **2007**, *9*, 222; h) T. Uemura, M. Ohba, S. Kitagawa, *Inorg. Chem.* **2004**, *43*, 7339 – 7345.

[15] J. M. Dominguez-Vera, E. Colacio, *Inorg. Chem.* **2003**, *42*, 6983 – 6985.

[16] J. G. Moore, E. J. Lochner, C. Ramsey, N. S. Dalal, A. E. Stiegman, *Angew. Chem.* **2003**, *115*, 2847 – 2849; *Angew. Chem. Int. Ed.* **2003**, *42*, 2741 – 2743.

[17] a) B. Folch, Y. Guari, J. Larionova, C. Luna, C. Sangregorio, C. Innocenti, A. Caneschi, C. Guérin, *New J. Chem.* **2008**, *32*, 273 – 282; b) G. Clavel, Y. Guari, J. Larionova, C. Guérin, *New J. Chem.* **2005**, *29*, 275 – 279.

[18] P. Zhou, D. Xue, H. Luo, X. Chen, *Nano Lett.* **2002**, *2*, 845 – 847.

[19] a) Y. Guari, J. Larionova, K. Molvinger, B. Folch, C. Guérin, *Chem. Commun.* **2006**, 2613 – 2615; b) Y. Guari, J. Larionova, M. Corti, A. Lascialfari, M. Marinone, G. Poletti, K. Molvinger, C. Guérin, *Dalton Trans.* **2008**, 3658 – 3660.

[20] G. Molnár, V. Niel, A. B. Gaspar, J.-A. Real, A. Zwick, A. Bousseksou, J. J. McGarvey, *J. Phys. Chem. B* **2002**, *106*, 9701 – 9707.

[21] S. Cobo, D. Ostrovskii, S. Bonhommeau, L. Vendier, G. Molnár, L. Salmon, K. Tanaka, A. Bousseksou, *J. Am. Chem. Soc.* **2008**, *130*, 9019 – 9024.

[22] a) R. Valentin, K. Molvinger, F. Quignard, D. Brunel, *New J. Chem.* **2003**, *27*, 1690 – 1692; b) K. Molvinger, F. Quignard, D. Brunel, M. Boissière, J.-M. Devoiselle, *Chem. Mater.* **2004**, *16*, 3367 – 3372.

[23] Note added in proof: Three reports on the synthesis of spin-crossover nanoparticles have appeared after this manuscript was submitted: a) I. Boldog, A. B. Gaspar, V. Martínez, P. Pardo-Ibañez, V. Ksenofontov, A. Battacharjee, P. Gütlich, J. A. Real, *Angew. Chem.* **2008**, *120*, 6533 – 6537; Angew. Chem. Int. Ed. **2008**, 47, 6433 – 6437; b) F. Volatron, L. Catala, E. Rivière, A. Gloter, O. Stéphan, T. Mallah, Inorg. Chem. **2008**, *47*, 6584 – 6586; c) T. Forestier, S. Mornet, N. Daro, T. Nishihara, S.-i. Mouri, K. Tanaka, O. Fouché, E. Freysz, J.-F. Létard, *Chem. Commun.* **2008**, 4327 – 4329.

 © 2008 Wiley-VCH Verlag GmbH & Co. KGaA, Weinheim